Title	Editing Light Emission with Stable Crystalline Covalent Organic Frameworks via Wall Surface Perturbation
Author(s)	Li, Zhongping; Geng, Keyu; He, Ting; Tan, Ke Tian; Huang, Ning; Jiang, Qiuhong; Nagao, Yuki; Jiang, Donglin
Citation	Angewandte Chemie international edition, 60(35): 19419-19427
Issue Date	2021-06-18
Type	Journal Article
Text version	author
URL	http://hdl.handle.net/10119/18091
Rights	This is the peer reviewed version of the following article: Copyright (C) 2021 Wiley-VCH. Zhongping Li, Keyu Geng, Ting He, Ke Tian Tan, Ning Huang, Qiuhong Jiang, Yuki Nagao, Donglin Jiang, Angewandte Chemie international edition, 60(35), 2021, pp.19419-19427, which has been published in final form at https://10.1002/anie.202107179. This article may be used for non-commercial purposes in accordance with Wiley Terms and Conditions for Use of Self-Archived Versions. This article may not be enhanced, enriched or otherwise transformed into a derivative work, without express permission from Wiley or by statutory rights under applicable legislation. Copyright notices must not be removed, obscured or modified. The article must be linked to Wiley's version of record on Wiley Online Library and any embedding, framing or otherwise making available the article or pages thereof by third parties from platforms, services and websites other than Wiley Online Library must be prohibited.
Description	

RESEARCH ARTICLE

Editing Light Emission with Stable Crystalline Covalent Organic Frameworks *via* Wall Surface Perturbation

Zhongping Li,[+] Keyu Geng,[+] Ting He, Ke Tian Tan, Ning Huang, Qiuhong Jiang, Yuki Nagao, and Donglin Jiang*

[a] Dr. Z. Li, [+] K. Geng,[+] Dr. T. He, K. T. Tan, Dr. N. Huang, Q. Jiang, Prof. Dr. D. Jiang*
Department of Chemistry, Faculty of Science, National University of Singapore
3 Science Drive 3, Singapore 117543, Singapore
E-mail: chmjd@nus.edu.sg
[b] Dr. Z. Li, Prof. Dr. Y. Nagao
Area of Materials Chemistry, School of Materials Science
Japan Advanced Institute of Science and Technology
1-1 Asahidai, Nomi, Ishikawa 923-1292, Japan
[c] Prof. Dr. D. Jiang*
Joint School of National University of Singapore and Tianjin University
International Campus of Tianjin University
Fuzhou 350207, China.
[+] These authors contributed equally to this work.

Supporting information for this article is given via a link at the end of the document.

Abstract: The ordered π skeletons of covalent organic frameworks make them viable light-emitting materials but their limited tunability has precluded further implementation. Here we report the synthesis of hydrazone-linked frameworks which are stable in water, acid, and base, and demonstrate their utility as a platform for light emission. The polygonal backbone is designed to be luminescent and partially π conjugated while the pore wall is docked with single atom or unit to induce resonance, hyperconjugation, and tautomerization effects. These effects can be transmitted to the backbone, so that the framework can emit three primary colors of light. The wall can be perturbated with multiple surface sites, rendering the material able to edit diverse emission colors in a predesignable and digital way. The systems show high activity, stability, tunability, and sensibility – a set of features attractive for light-emitting and sensing applications.

Introduction

Light emission is necessary for daily life and has broad applications in cutting-edge science and technology.[1] Red, green, and blue (RGB) are three primary colors of light and constitute the basis for organizing various lightening systems. Owing to a big difference in band gap, RGB emissions are usually obtained with different materials. If a material could systematically shift its band gap to emit RGB lights upon structural perturbation, this would be an ideal platform for designing light emission. However, exploring such a material is challenging as emission is determined by excited and ground states which are associated with materials' inherent electronic structures. An exceptional example is zero-dimensional (0D) quantum dot which can trigger size confinement effect, leading to size-dependent RGB emissions.[2] In contrast, organic/polymeric materials hardly develop such a system as π conjugation in polymers tends to saturate within a few repeating units, precluding the possibility of RGB emissions by tuning molecular length of the same π backbones.[3] In this work, we show an approach to tunable light emission based on an organic/polymeric system with a two-dimensional (2D) backbone.

Covalent organic frameworks (COFs) are a class of crystalline porous polymers which enable the integration of chromophores into well-defined 2D polygonal skeletons connected with different linkages.[4-6] With the ordered chromophore structures, COFs could construct light-emitting materials but their limited stability and tunability have precluded implementation.[7] Herein, we report COFs as a platform for editing light emission. This is based on our concept that surface groups on the pore wall can trigger distinct electronic effects which can be transmitted to the polygonal backbone so that the electronic structure of the whole framework is controlled by the surface sites. Unexpectedly, we observed that the framework enables a drastic change in electronic structure to afford RGB emissions by a small perturbation of single surface site. Surprisingly, integrating multicomponent surface sites onto the pore walls yields light-emitting materials and enables to edit tailor-made emission colors. We emphasize that unlike quantum dots which must change the particle size for a different emission, COFs do not need to alter the backbone size but can edit different colors *via* surface site perturbation in a predesignable and digital way. The systems exhibited high luminescence activity, stability, color tunability, and guest sensibility – a combination of features highly desired for light-emitting and sensing implementations. These results demonstrate a new regime for light emission.

Results

Design principle. We selected COFs as the platform for light emission as they enable the construction of extended polygonal backbones with well-defined structures. The COF architecture develops ordered π backbones and orientated one-dimensional (1D) channels *via* π-π stacking.[5a, 5b] One distinct feature is that

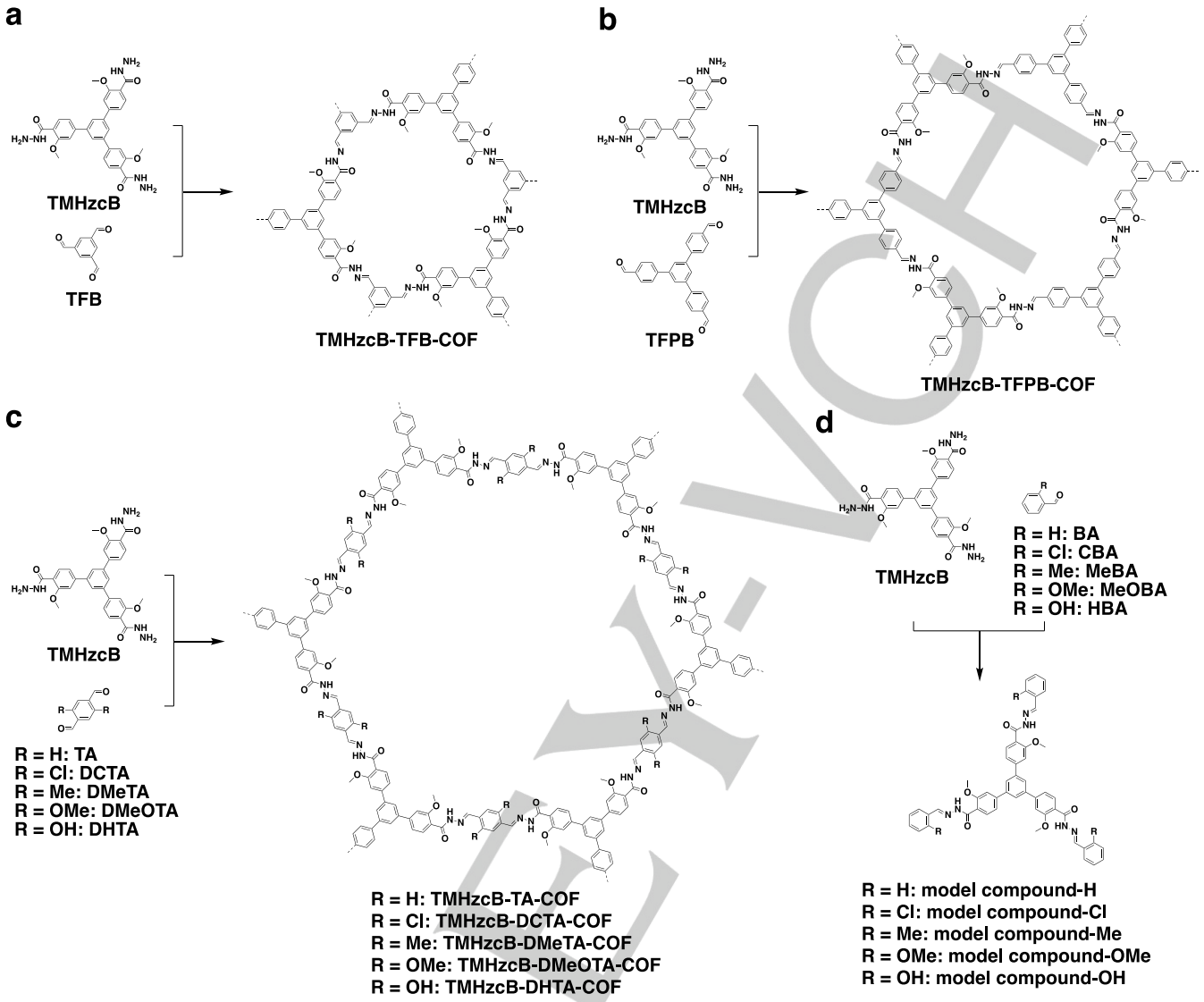

Figure 1. a) Schematic of TMHzcB-TFB-COF. b) Schematic of TMHzcB-TFPB-COF. c) Schematics of hydrazone-linked light-emitting COFs perturbated with different wall surface sites for editing light emission. d) Schematics of model compounds.

the 2D polygonal backbone can be easily engineered at molecular level to decorate different single atoms or units on pore walls. The surface site can trigger different π electronic interplays and transmits the effect to the backbone, offering a way to control the electronic structure of the whole framework. These features pave the chemical basis for editing light emission *via* simple wall surface perturbation. Integrating intra- or inter-layer hydrogen-bonding interactions could tune π distance, which however has a limited influence on the band gap and emission color.[8]

Distinct from non- or fully-conjugated linkage, hydrazone is unique as it allows p–π conjugation between the partially conjugated aryl amide bond and lone pair of linked nitrogen site, so that the knot and linker units are partially conjugated.[9] In this case, the surface site on the pore wall would have a chance to affect the p–π conjugation of the polygonal backbone and change its π electronic structure. We introduced single chlorine, methyl, methoxy, and hydroxy sites onto the pore wall (Figure 1), which are designed to trigger different interplays with the polygonal backbone *via* resonance, hyperconjugation, and phototautomerization effects. Dramatically, the polygonal backbones with different surface atom or site can emit three primary colors of light. More importantly, this strategy enables the wall surface perturbation with multiple atoms and sites to achieve tailor-made emission colors in a predesignable and digital way while retaining the same backbone.

Synthesis and characterization. We synthesized a set of newly designed hydrazone-linked COFs (Figures 1a–c), by polycondensation of 1,3,5-tris(3'-methoxy-4'-hydrazinecarbonylphenyl)benzene (TMHzcB) as a knot with 1,3,5-triformylbenzene (TFB), 1,3,5-tris(4-formylphenyl) benzene (TFPB), terephthalaldehyde (TA), 2,5-dichloroterephthalaldehyde (DCTA), 2,5-dimethylterephthalaldehyde (DMeTA), 2,5-dimethoxyterephthalaldehyde (DMeOTA), or 2,5-dihydroxyterephthalaldehyde (DHTA) as a linker under solvothermal conditions (for details see Supporting Information, Experimental Procedures). These reactions produce TMHzcB-

TFB-COF (Figure 1a), TMHzcB-TFPB-COF (Figure 1b), TMHzcB-TA-COF, TMHzcB-DCTA-COF, TMHzcB-DMeTA-COF, TMHzcB-DMeOTA-COF, and TMHzcB-DHTA-COF (Figure 1c) in 87%, 89%, 85%, 90%, 92%, 93%, and 89% yield, respectively. Among the series, TMHzcB-TFB-COF and TMHzcB-TFPB-COF serve as controls with only one hydrazone linkage at each edge, to see how the polygonal backbone itself affects light emission. The TMHzcB-TA-COF, TMHzcB-DCTA-COF, TMHzcB-DMeTA-COF, TMHzcB-DMeOTA-COF, and TMHzcB-DHTA-COF (Figure 1c) possess two hydrazone linkages at each edge, and they are identical in the polygonal backbone but have different wall surface sites (R), i.e. hydrogen, chlorine, methyl, methoxy, and hydroxy, respectively (Figure 1c). Moreover, five model compounds, i.e. model compound-H, model compound-Cl, model compound-Me, model compound-OMe, and model compound-OH were used to distinguish the knot and linker effects (Figure 1d).

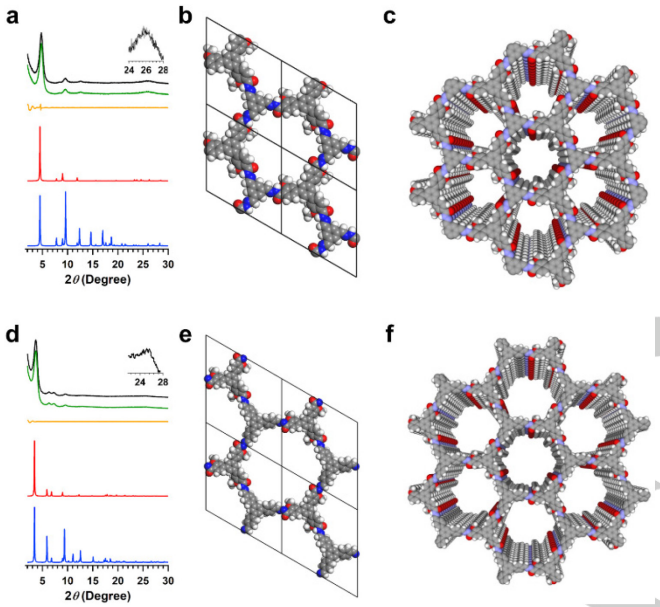

Figure 2. Crystal structures of blue light-emitting COFs. a) PXRD patterns of experimentally observed (black curve), Pawley refined (green curve) and their difference (orange curve), and simulated from the eclipsed AA-stacking mode (red curve) and staggered AB-stacking mode (blue curve) of TMHzcB-TFB-COF. b) Unit cell of TMHzcB-TFB-COF. c) Reconstructed 10 layers of TMHzcB-TFB-COF (seven pores are shown). d) PXRD patterns of experimentally observed (black curve), Pawley refined (green curve), and their difference (orange curve), and simulated from the eclipsed AA-stacking mode (red curve) and staggered AB-stacking mode (blue curve) of TMHzcB-TFPB-COF. e) Unit cell of TMHzcB-TFPB-COF. f) Reconstructed 10 layers of TMHzcB-TFPB-COF (seven pores are shown).

Fourier transform infrared (FT IR) spectroscopy revealed the stretching vibrations of the C=N bond in the hydrazone linkage at 1665–1686 cm^{-1}, which are close to those of their corresponding model compounds (Figure S1). Field emission scanning electron microscopy showed polymeric morphologies (Figure S2). Elemental analysis confirmed that the C, H, and N contents are close to the theoretical values (Table S1). Thermogravimetric analysis revealed that these COFs do not lose weight up to 300 °C under N_2 (Figure S3).

Crystal structures. The TMHzcB-TFB-COF exhibited powder X-ray diffraction (PXRD) peaks at 4.78°, 8.32°, 9.56°, 12.71°, and 25.71°, which were assigned to the (100), (110), (200), (210), and (001) facets (Figure 2a, black curve), respectively. On the other hand, TMHzcB-TFPB-COF with a slightly bigger lattice displayed PXRD peaks at 3.65°, 6.31°, 7.25°, 9.54°, and 25.43°, which were assigned to the (100), (110), (200), (210), and (001) facets, respectively (Figure 2d, black curve).

The TMHzcB-TA-COF (Figure 3a, black curve), TMHzcB-DCTA-COF (Figure 3d, black curve), TMHzcB-DMeTA-COF (Figure 3g, black curve), TMHzcB-DMeOTA-COF (Figure 3j, black curve), and TMHzcB-DHTA-COF (Figure 3m, black curve) exhibited similar PXRD patterns to each other, to have peak sets of [2.34° (100), 4.08° (110), 6.42° (210), and 25.53° (001)], [2.36° (100), 4.09° (110), 4.74° (200), 6.26° (210), 8.40° (310), and 26.02° (001)], [2.40° (100), 4.26° (110), 4.94° (200), 6.49° (210), 8.68° (310), and 26.24° (001)], [2.56° (100), 4.98° (110), 6.70° (210), 8.94° (310), and 26.76° (001)], and [2.38° (100), 4.90° (110), 8.26° (210), and 26.30° (001)], respectively. Pawley refinements of these seven COFs (Figures 2a, 2d, 3a, 3d, 3g, 3j, and 3m, green curves) confirmed the peak assignments as evidenced by negligible differences (Figures 2a, 2d, 3a, 3d, 3g, 3j, and 3m, orange curves).

Structural simulations using density function tight binding (DFTB+) revealed that the AA stacking mode (for atomistic coordinates see Supporting Information, Tables S2–S8) reproduced the experimentally observed PXRD patterns (Figures 2a, 2d, 3a, 3d, 3g, 3j, and 3m, red curves). In contrast, the AB stacking mode does not match the experimental results (Figures 2a, 2d, 3a, 3d, 3g, 3j, and 3m, blue curves). Therefore, these COFs constituted extended 2D hexagonal lattices (Figures 2b, 2e, 3b, 3e, 3h, 3k, and 3n), which further stack to form layer frameworks (Figures 2c, 2f, 3c, 3f, 3i, 3l, and 3o). Moreover, the (001) facets at 25.43°–26.76° correspond to small interlayer intervals of 3.50–3.33 Å, suggesting that the surface sites are dense aligned on the pore wall. The well-defined organization of surface sites is unique, which can hardly be achieved in conventional organic/polymeric materials.

Porosity. The TMHzcB-TFB-COF is microporous to exhibit type-I N_2 sorption isotherm (Figure S4a) and possesses a Brunauer–Emmett–Teller (BET) surface area of 471 $m^2\ g^{-1}$ with a pore size of 1.6 nm and a pore volume of 0.23 $cm^3\ g^{-1}$ (Figure S4b). The TMHzcB-TFPB-COF has a BET surface area of 1116 $m^2\ g^{-1}$, a pore size of 2.1 nm, and a pore volume of 0.52 $cm^3\ g^{-1}$ (Figures 4c and 4d). The TMHzcB-TA-COF (Figures 4e and 4f), TMHzcB-DCTA-COF (Figures 4g and 4h), TMHzcB-DMeTA-COF (Figures 4i and 4j), TMHzcB-DMeOTA-COF (Figures 4k and 4l), and TMHzcB-DHTA-COF (Figures 4m and 4n) are mesoporous and exhibit a BET surface area of 470, 1082, 932, 799, and 342 $m^2\ g^{-1}$, respectively. Their pore sizes are 3.7, 3.7, 3.7, 3.2, and 3.6 nm, while pore volumes are 0.26, 0.72, 0.56, 0.39, and 0.21 $cm^3\ g^{-1}$, respectively (Figure S4).

Stability. We investigated stability by dispersing COFs in tetrahydrofuran (THF), water, hydrochloric acid (HCl, 1 M), and aqueous sodium hydroxide solution (NaOH, 1 M or 0.1 M), respectively, at 25 °C for 24 h. These COFs retained PXRD peaks, suggesting the robustness of the polygonal backbone (Figure S5).

Electronic abstraction features. We measured diffuse reflectance Kubelka−Munk (K–M) spectra of COFs, building units and model compounds in the solid state (Table 1, Figure S6, and Table S9) to reveal their electronic absorption features. Model compound-H, model compound-Cl, model compound-Me, model compound-OMe, and model compound-OH exhibited absorption

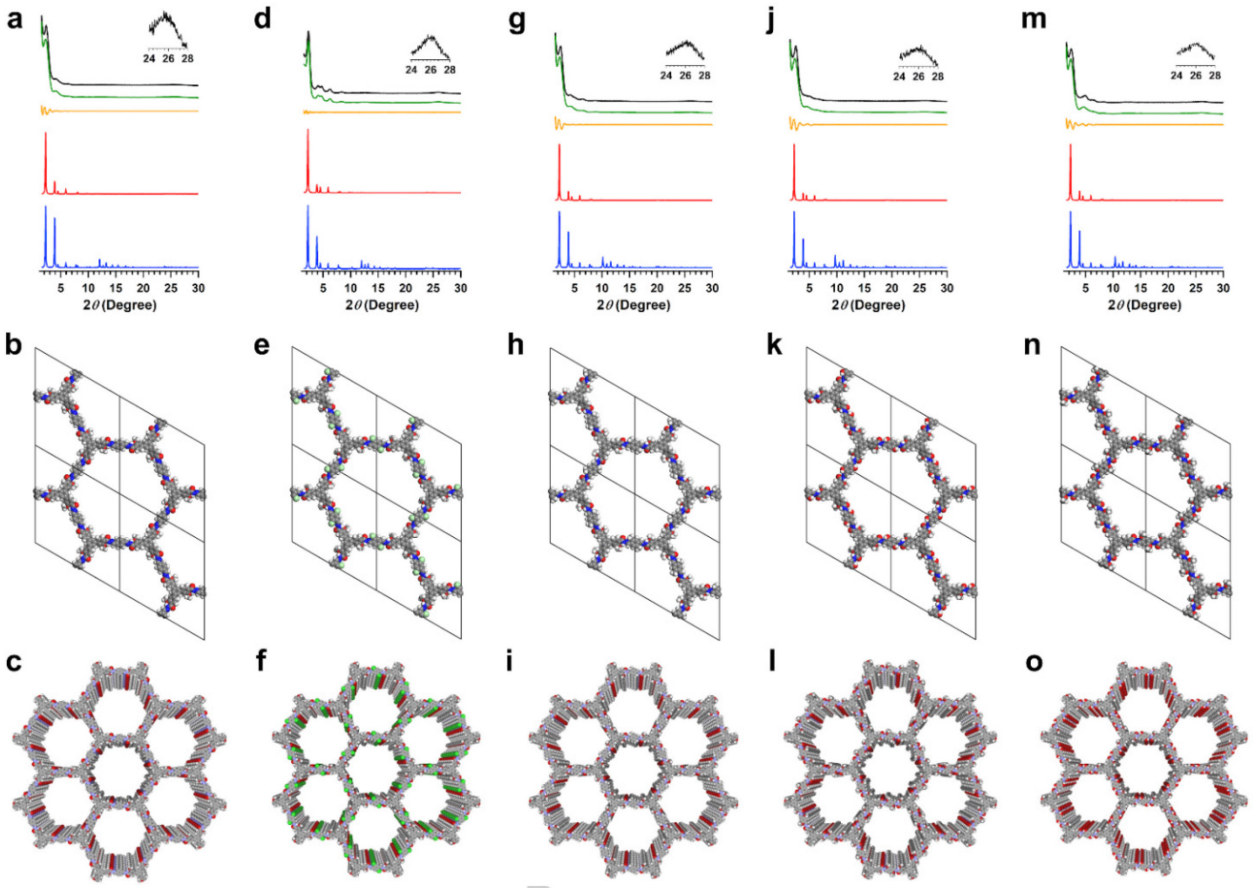

Figure 3. Crystal structures of surface-perturbated COFs for RGB emissions. (a, d, g, j, and m) PXRD patterns of experimentally observed (black curves), Pawley refined (green curves) and their difference (orange curves), and simulated from the eclipsed AA-stacking mode (red curves) and staggered AB-stacking mode (blue curves), of (a) TMHzcB-TA-COF, (d) TMHzcB-DCTA-COF, (g) TMHzcB-DMeTA-COF, (j) TMHzcB-DMeOTA-COF, and (m) TMHzcB-DHTA-COF, respectively. (b, e, h, k, and n) Unit cell of (b) TMHzcB-TA-COF, (e) TMHzcB-DCTA-COF, (h) TMHzcB-DMeTA-COF, (k) TMHzcB-DMeOTA-COF, and (n) TMHzcB-DHTA-COF, respectively. (c, f, i, l, and o) Reconstructed 10 layers of (c) TMHzcB-TA-COF, (f) TMHzcB-DCTA-COF, (i) TMHzcB-DMeTA-COF, (l) TMHzcB-DMeOTA-COF, and (o) TMHzcB-DHTA-COF, respectively (seven pores are shown).

bands at 366, 364, 368, 367, and 370 nm, respectively (Figures S6a–g, black curves, Table S9). The small difference suggests that the surface site has a limited effect on the model compounds.

The TMHzcB-TFB-COF (Table 1, Figure S6a, red curve) and TMHzcB-TFPB-COF (Table 1, Figure S6b, red curve) exhibited absorption bands at 380 and 390 nm, respectively, which are clearly redshifted from those of TMHzcB (blue curves, 327 nm), TFB (green curves, 357 nm), and model compound-H (black curves, 366 nm; Table S9). These redshifts suggest the extension of conjugation in the polygonal backbone.

The TMHzcB-TA-COF with surface H atom exhibited an absorption band at 387 nm (Table 1, Figure S6c, red curve). The TMHzcB-DCTA-COF with surface Cl atom (Table 1, Figure S6d, red curve) exhibited an adsorption band at 406 nm, which is greatly redshifted by 42 nm from model compound-Cl and by 19 nm from TMHzcB-TA-COF. The Cl atom triggers inductive effect owing to its electronegativity which reduces the π density of p–π conjugated edge while the lone pairs of Cl donate electrons to the edge to increase the π density. The progressed redshift reflects that the p–π conjugation in TMHzcB-DCTA-COF is extended by the Cl atom. Thus, the resonance effect of Cl atom is predominant in the framework (Figure 4a).

The TMHzcB-DMeTA-COF with methyl surface site exhibited an absorption band at 414 nm (Table 1, Figure 6e, red curve), which is redshifted by 46 and 8 nm from model compound-Me and TMHzcB-DCTA-COF, respectively. These redshifts indicate a further progressed p–π conjugation compared to those of TMHzcB-DCTA-COF with surface Cl atom and TMHzcB-TA-COF bearing surface H atom. The methyl group can trigger hyperconjugation *via* its C–H bonds, which donate electron to the edge to enhance its p–π conjugation (Figure 4b). More explicitly, integrating methoxy site onto the wall further induces progressed redshift of absorption band because of improved p–π conjugation driven by the resonance effect of lone pairs of O atoms (Figure 4c). Indeed, TMHzcB-DMeOTA-COF (Table 1, Figure S6f, red curve) exhibited the absorption band at 441 nm, which is 74- and 27-nm redshifted from those of model compound-OMe and TMHzcB-DMeTA-COF, respectively.

Similarly, TMHzcB-DHTA-COF with hydroxy unit exhibited an absorption band at 453 nm (Table 1, Figure 6g, red curve), which is 83- and 12-nm redshifted from those of model compound-OH and TMHzcB-DMeOTA-COF, respectively. The progressed redshifts originate from a two-fold effect: one is the resonance effect of the O atom, and another is the improved planarity of

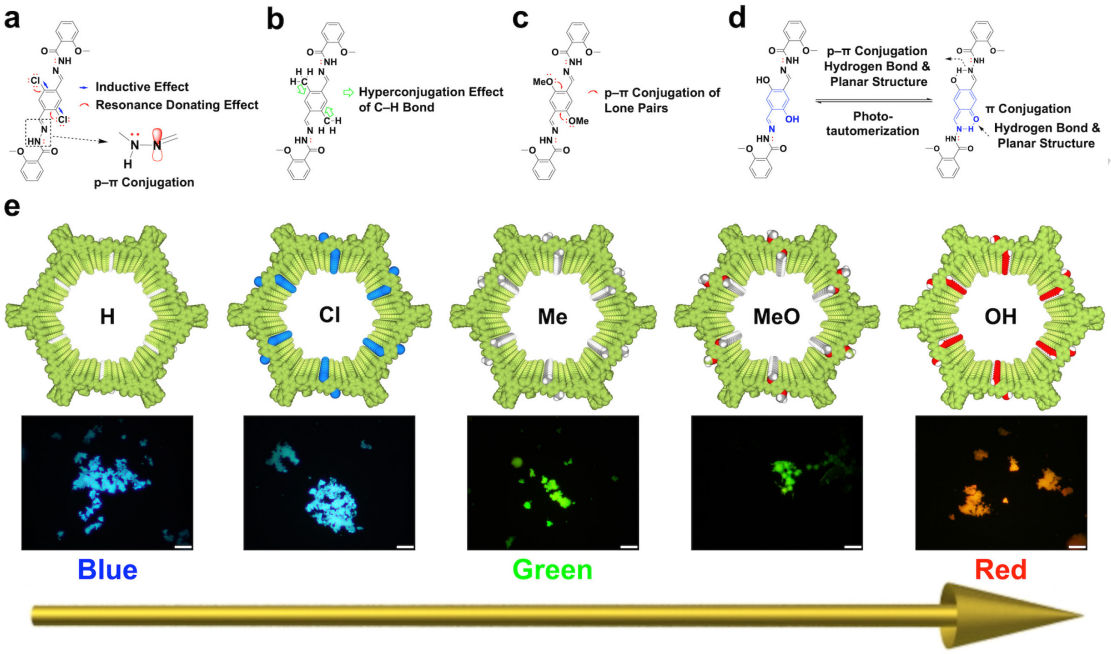

Figure 4. Perturbation of surface site and their effects. (a–d) Electronic effects of (a) Cl atom *via* induction and resonance (inset: p–π conjugation of hydrazone linkage), (b) methyl site *via* hyperconjugation, (c) methoxy site *via* resonance, and (d) hydroxyl site *via* hydrogen bond and phototautomerization, on the backbone. e) Progress of light emission *via* perturbation of wall surface site, enabling to emit three primary colors and to edit different light emissions (scale bar = 20 μm).

linker *via* hydrogen bond interaction between the hydroxy unit and hydrazone linkage (Figure 4d).

The drastic changes in the absorption band of these COFs reveal that the surface sites play a key role in controlling the p–π conjugation of the polygonal backbone (Figures 4a–d). Each macrocycle possesses six surface sites which are aligned along the z direction to form six single file chains in each channel (Figures 3c, 3f, 3i, 3l, and 3o). Therefore, the effect of these surface chains can be transmitted to the polygonal backbone to influence the p–π conjugation and electronic structure.

Emission of RGB lights. The distinct electronic effects attracted us to investigate light emission behavior of COFs, upon excitation at their absorption bands. Model compound-H, model compound-Cl, model compound-Me, model compound-OMe, and model compound-OH emitted at 406, 435, 442, 445, and 528 nm, respectively (Figure S7, Table S9). Both COFs with one hydrazone linkage at each edge emitted blue light. For example, TMHzcB-TFB-COF emits at 447 nm (Figure 5a) with an absolute fluorescence quantum yield of 5.1% (Figure 5b) and the standard Commission Internationale de l'Eclairage (CIE) coordinate of (0.15, 0.03) (Table 1, Figure 5c). The TMHzcB-TFPB-COF emitted at 469 nm (Figure 5a) with a quantum yield of 10.5% (Figure 5b) and a CIE coordinate of (0.12, 0.12) (Figure 5c).

The TMHzcB-TA-COF with surface H atom also emitted a blue light at 463 nm (Figure 5a) with a quantum yield of 11.7% (Figure 5b) and a CIE coordinate of (0.14, 0.06) (Table 1, Figure 5c). On the other hand, TMHzcB-DCTA-COF with surface Cl atom emitted a sky-blue light at 482 nm (Figure 5a) with an absolute quantum yield of 6% (Figure 5b) and a CIE coordinate of (0.11, 0.20) (Table 1, Figure 5c). Interestingly, TMHzcB-DCTA-COF exhibited a similar redshift by 19 nm in both absorption and emission bands compared to those of TMHzcB-TA-COF. This result suggests that the Cl atom controls the emission *via* its resonance effect.

Interestingly, TMHzcB-DMeTA-COF with surface methyl site exhibited a further redshifted luminescence to emit green at 499 nm (Figure 5a) with a quantum yield of 20% (Figure 5b) and a CIE coordinate of (0.13, 0.45) (Table 1, Figure 5c). This redshift originates from the hyperconjugation effect of the methyl site (Figure 4c). The high fluorescence quantum yield is compatible to the state-of-the-art COFs represented by TPE-Ph COF (32%),[10a] sp2c-COF (14%),[10b] and 3D-TPE-COF (20%).[10c] Notably, distinct from aggregation-induced emission of backbones in these COFs, the emission of our newly designed COFs is controlled by the surface site on the pore wall (Figure 4d).

The TMHzcB-DMeOTA-COF with surface methoxy site also emitted a green light with a redshifted band at 526 nm (Figure 5a) and exhibited an absolute quantum yield of 19% (Figure 5b) and a CIE coordinate of (0.17, 0.74) (Table 1, Figure 5c). These results indicate that the resonance effect of methoxy site drives the redshift of both absorption and emission bands (Figure 4c).

Surprisingly, TMHzcB-DHTA-COF with surface hydroxyl site emitted a red light centered at 635 nm (Figure 5a) to achieve a quantum yield of 3.1% (Figure 5b) and a CIE coordinate of (0.69, 0.31) (Table 1, Figure 5c). At the ground state, TMHzcB-DHTA-COF exists in the stable enol form.[11] Photoexcitation induces the redistribution of electron density to increase the acidity of the hydrogen bond donor (−OH) and the basicity of the hydrogen bond acceptor (=N−). As a result, phototautomerization occurs to transform enol to keto form, yielding an exited keto form (Figure 4d).[11] This phototautomerization effect makes TMHzcB-DHTA-COF distinct from red emissive porphyrin COFs as the surface site of new COFs induces a red emission (Figure 4d).[8a, 12]

Compared to model compounds, the emission band of COFs is greatly redshifted by 60–100 nm (Table 1), suggesting the importance of surface site on the polygonal backbone. The dense yet aligned surface sites form multipoint and multichain on the

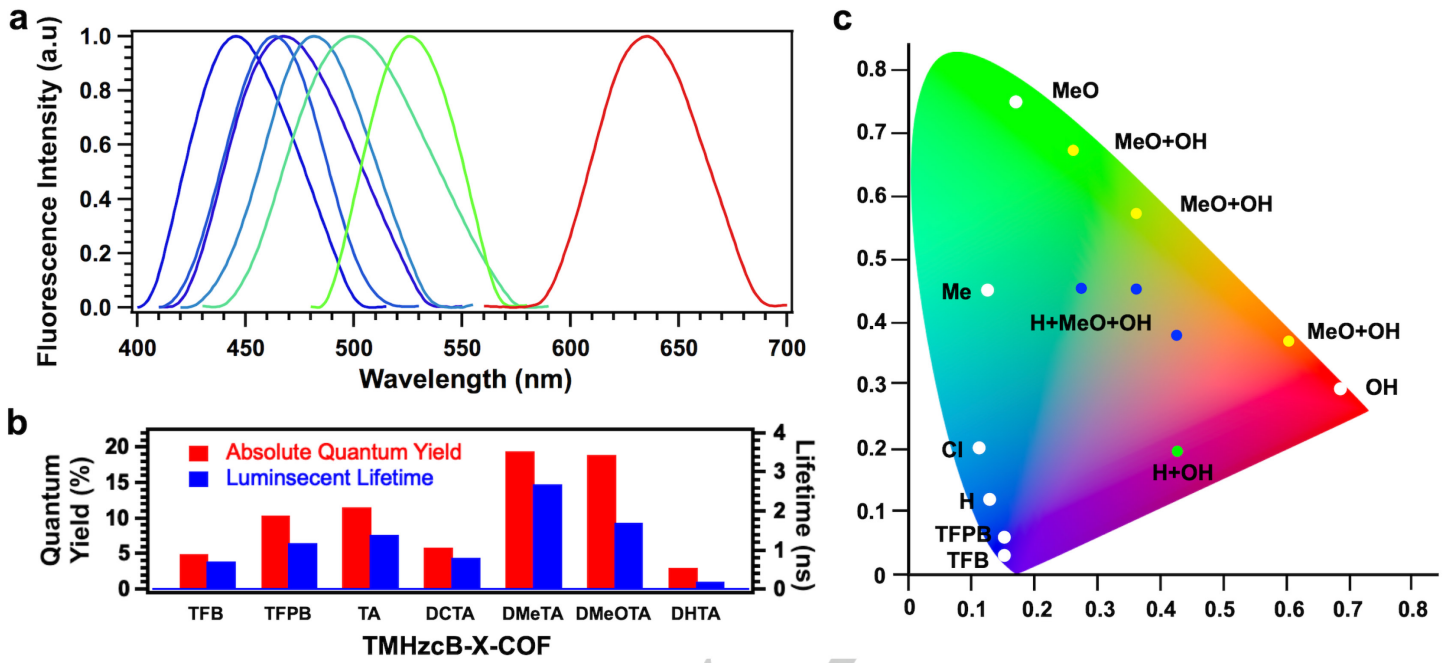

Figure 5. Editing light emission via surface perturbation. a) Fluorescence spectra of TMHzcB-TFB-COF, TMHzcB-TA-COF, TMHzcB-TFPB-COF, TMHzcB-DCTA-COF, TMHzcB-DMeTA-COF, TMHzcB-DMeOTA-COF, and TMHzcB-DHTA-COF at solid state (normalized peak top from left to right). b) Absolute fluorescence quantum yield (red bar) and lifetime (blue bar) of TMHzcB-X-COF (X = TFB, TFPB, TA, DCTA, DMeTA, DMeOTA, and DHTA). c) CIE coordinates of COFs perturbated with single surface site (white dots), two surface sites (yellow and green dots), and three surface sites (blue dots).

six walls of each channel, so that the resonance, hyperconjugation, and phototautomerization effects are collectively and sensitively transmitted to the photoexcited state. These features render the backbone able to emit different lights (Table 1, Figures 4e and 5c).

Stokes shift. To probe how the surface site influences vibrational states, we evaluated Stokes shift to show the energy differences between the absorption and emission bands of the COFs. As a result, the Stokes shift follows an order of TMHzcB-DHTA-COF (6327 cm^{-1}) > TMHzcB-TFPB-COF (4319 cm^{-1}) > TMHzcB-TA-COF (4241 cm^{-1}) > TMHzcB-DMeTA-COF (4114 cm^{-1}) > TMHzcB-TFB-COF (3944 cm^{-1}) > TMHzcB-DCTA-COF (3883 cm^{-1}) > TMHzcB-DMeOTA-COF (3664 cm^{-1}). We further measured time-resolved fluorescence spectra to evaluate the fluorescence lifetime (Figure 5b, Figure S8). Indeed, TMHzcB-DHTA-COF with the largest Stokes shift exhibited the shortest fluorescence lifetime (0.21 ns, Figure 5b, Figure S8), while TMHzcB-DMeOTA-COF with the resonance effect and TMHzcB-DMeTA-COF with hyperconjugation effect displayed much longer lifetimes of 1.71 and 2.71 ns, respectively (Figure 5b, Figure S8). According to Perrin-Jablonski diagram and Frank-Cotton principle, the difference in Stokes shifts and fluorescence lifetimes are self-consistent and reflect that the surface site plays a critical role in phonon relaxation, which triggers the difference of light emission.

Discussion

With the development of three primary colors of light, we scrutinized the possibility of editing light emission. As linker units have different surface sites, developing multicomponent linkers to conduct polycondensation reaction enables the perturbation of wall surface with different sites while retaining the same polygonal backbone. This approach would produce emission colors that are distinct from those with single surface site.

We first challenged to edit light emission between green and red by synthesizing TMHzcB-DMeOTA$_X$/DHTA$_Y$-COFs with two surface sites, i.e. methoxy and hydroxy sites at different molar ratios (X/Y = 2/1, 1/1, and 1/2 in mol) by polycondensation of TMHzcB as knot with a mixture of DMeOTA and DHTA as linker (for details see Supporting Information, Experimental Procedures). The TMHzcB-DMeOTA$_X$/DHTA$_Y$-COFs were characterized by FT IR spectroscopy (Figure S9), elemental analysis (Table S1), PXRD (Figure S10), and nitrogen sorption isotherm measurements (Figure S11). The TMHzcB-DMeOTA$_X$/DHTA$_Y$-COFs exhibited absorption bands at 450, 450, and 440 nm as the X/Y ratio was changed from 2/1 to 1/1 and 1/2 (Table 1, Figures S12a–c). Interestingly, upon excitation at their absorption bands, TMHzcB-DMeOTA$_X$/DHTA$_Y$-COFs showed dual emission bands at 517 and 640 nm; each band is close to that of TMHzcB-DMeOTA-COF and TMHzcB-DHTA-COF, respectively (Table 1, Figures S12a–c). The TMHzcB-DMeOTA$_2$/DHTA$_1$-COF, TMHzcB-DMeOTA$_1$/DHTA$_1$-COF, and TMHzcB-DMeOTA$_1$/DHTA$_2$-COF exhibited a CIE coordinate of (0.22, 0.66), (0.37, 0.54), and (0.60, 0.39), respectively (Table 1, Figure 5c, yellow spots). Clearly, the emission colors are distinct from the COFs with single surface site. Looking closely at the CIE plot, we found that the spots of these COFs with two surface sites are aligned between the spots of green shining TMHzcB-DMeOTA-COF and red emissive TMHzcB-DHTA-COF (Figure 5c).

We then edited the emission color between blue and red by engineering the wall surface with proton and hydroxyl sites to produce TMHzcB-TA$_2$/DHTA$_1$-COF (Table S1, Figures S9-S11),

Table 1. Absorption and emission features of COFs.

Single surface site COFs	Abs. (nm)	Em. (nm)	CIE coordinate	Multiple surface site COFs	Molecular Ratio	Abs. (nm)	Em. (nm)	CIE coordinate
TMHzcB-TFB-COF	380	447	(0.15, 0.03)	TMHzcB-DMeOTA$_X$/DHTA$_Y$-COFs	X/Y = 2/1	450	517 and 640	(0.22, 0.66)
TMHzcB-TFPB-COF	390	469	(0.12, 0.12)		X/Y = 1/1	450		(0.37, 0.54)
TMHzcB-TA-COF	387	463	(0.14, 0.06)		X/Y = 1/2	440		(0.60, 0.39)
TMHzcB-DCTA-COF	406	482	(0.11, 0.20)	TMHzcB-TA$_X$/DHTA$_Y$-COF	X/Y = 2/1	440	468 and 638	(0.42, 0.18)
TMHzcB-DMeTA-COF	414	499	(0.13, 0.45)	TMHzcB-TA$_X$/DMeOTA$_Y$/DHTA$_Z$-COFs	X/Y/Z = 3/1/2	448	468, 533, and 640	(0.29, 0.46)
TMHzcB-DMeOTA-COF	441	526	(0.17, 0.74)		X/Y/Z = 2/1/2	456		(0.34, 0.46)
TMHzcB-DHTA-COF	453	635	(0.69, 0.31)		X/Y/Z = 4/1/4	442		(0.42, 0.38)

as TMHzcB-TA-COF and TMHzcB-DHTA-COF emit blue and red, respectively. The TMHzcB-TA$_2$/DHTA$_1$-COF upon excitation at 440 nm affords a dual luminescence at 468 and 638 nm (Table 1, Figure S12d), which is again close to the emission band of TMHzcB-TA-COF and TMHzcB-DHTA-COF, respectively. The TMHzcB-TA$_2$/DHTA$_1$-COF exhibited a CIE coordinate of (0.42, 0.18) (Table 1, Figure 5c, green spot), which is spotted between TMHzcB-TA-COF and TMHzcB-DHTA-COF. These results are indicative as the emission color can be predesigned by solely tuning the ratio of surface sites on the pore wall.

We further perturbate the frameworks with three surface sites. For this purpose, we selected TMHzcB as knot and three linkers of TA, DMeOTA, and DHTA for the polymerization. We tuned the molar ratio of TA/DMeOTA/DHTA at 3/1/2, 2/1/2, and 4/1/4 to synthesize three COFs, i.e. TMHzcB-TA$_3$/DMeOTA$_1$/DHTA$_2$-COF, TMHzcB-TA$_2$/DMeOTA$_1$/DHTA$_2$-COF, and TMHzcB-TA$_4$/DMeOTA$_1$/DHTA$_4$-COF, respectively (Table S1, Figures S9–S11). All TMHzcB-TA$_3$/DMeOTA$_1$/DHTA$_2$-COF, TMHzcB-TA$_2$/DMeOTA$_1$/DHTA$_2$-COF, and TMHzcB-TA$_4$/DMeOTA$_1$/DHTA$_4$-COF exhibited three emission bands at 468, 533, and 640 nm (Table 1, Figure S13), which is close to the blue, green, and red luminescence of TMHzcB-TA-COF, TMHzcB-DMeOTA-COF, and TMHzcB-DHTA-COF (Table 1), respectively. Interestingly, the intensity of three emissions is different from each other, so that the emission color of these COFs is finely controlled by the molar ratio of surface sites. Indeed, TMHzcB-TA$_3$/DMeOTA$_1$/DHTA$_2$-COF, TMHzcB-TA$_2$/DMeOTA$_1$/DHTA$_2$-COF, and TMHzcB-TA$_4$/DMeOTA$_1$/DHTA$_4$-COF exhibited different CIE coordinates of (0.29, 0.46), (0.34, 0.46), and (0.42, 0.38), respectively (Table 1, Figure 5c, blue spots).

As demonstrated above, our strategy can edit light emission in a predesignable and digital way by tuning the component and ratio of surface sites. Synthetically, any colors in the CIE diagram surrounded by these five COFs can be predesigned by engineering the surface sites. Such an editing capability is unprecedented in both organic and inorganic systems. We highlight that distinct from 0D quantum dots which must change the particle size, the 2D COFs do not need to alter the backbone but can emit various lights by simply decorating different surface sites. Therefore, our strategy offers a new regime in light-emitting materials.

Hydrazone serves as a hydrogen-bond acceptor owing to the presence of N and O atoms with lone pairs. We observed that the hydrazone linkages endow these light-emitting COFs with exceptional sensing capability. We proved the concept by using TMHzcB-DMeTA-COF with the highest fluorescence quantum yield to probe 2,4,6-trinitrophenol (TNP) in THF. A drastic and quick drop of fluorescence was observed (Figure S14a and inset). Noticeably, the detection limit is as low as sub ppm level; this high sensitivity is much superior to the reported COFs.[13] The TMHzcB-DMeTA-COF is highly selective in sensing and shows a low quenching degree by other aromatic compounds even at much higher concentrations (Figure S14b), including 2,4-dinitrophenol (DNP, quenching degree = 16%), 2,4-dinitrotoluene (DNT, quenching degree = 7%), 2-nitrophenol (NP, quenching degree = 5%), and 2-nitrotoluene (NT, quenching degree = 4%).

From the fluorescence quenching profile, the Stern–Volmer constant (K_{SV}) was evaluated to be 3.7 × 10^5 M^{-1} (Figure S14c). Time-resolved fluorescence decay measurements revealed that the lifetime of TMHzcB-DMeTA-COF in THF was 2.10 ns (Figure S14d, black curve) which decreased to 1.49 ns upon addition of TNP (10 ppm) (Figure S14d, blue curve). This result indicates that photoinduced electron transfer proceeds at a rate of 1.9 × 10^8 s^{-1} and controls the sensing process. The fluorescence quenching rate constant k_q (= K_{SV} / τ) was evaluated to be as high as 2.5 × 10^{14} M^{-1} s^{-1}. Therefore, the hydrazone-linked COF merges selectivity, sensitivity, and sensibility into one material, which is highly desired for sensors and detectors.

Conclusion

In summary, we have developed COFs as a molecular platform for editing light emission. This is possible by integrating hydrogen, chlorine, methoxy, methyl, and hydroxy surface sites onto the pore wall, which are designed to trigger various π electronic effects including resonance, hyperconjugation, and phototautomerization. The surface site transmits the effect to the polygonal backbone, so that the ground and excited states can induce a drastic change to emit three primary colors of light. The multiple surface site perturbation approach greatly increases the scope of emission colors and enable to edit diverse light emissions in a predesignable and digital way. The frameworks combine luminescence activity, stability, color tunability, and sensibility in one material which is highly desired for light-emitting and sensing applications. With the diversity of polygonal topology as well as the broad scope of backbone and surface site, we envision that our strategy shapes a new regime in light-emitting organic/polymeric materials.

Acknowledgements

This work is supported by the MOE tier 1 grant (R-143-000-A71-114) and NUS start-up grant (R-143-000-A28-133).

Conflict of interest

The authors declare no conflict of interests

Keywords: covalent organic framework • hydrazone linkage • luminescence • color design • RGB

[1] C.R. Ronda, Luminescence: from theory to applications. John Wiley & Sons, **2007**.

[2] a) D.J. Norris, M.G. Bawendi, *Phys. Rev.* B **1996,** *53*, 16338; b) T. Takagahara, K. Takeda, *Phys. Rev.* B **1992,** *46*, 15578.

[3] A. Haque, R. A. Al-Balushi, I. J. Al-Busaidi, M.S. Khan, P.R. Raithby, *Chem. Rev.* **2018,** *118*, 8474−8597.

[4] a) E. Jin, M. Asada, Q. Xu, S. Dalapati, M. A. Addicoat, M. A. Brady, H. Xu, T. Nakamura, T. Heine, Q. Chen, D. Jiang, *Science* **2017**, *357*, 673–676; b) T. Ma, E. A. Kapustin, S. Yin, L. Liang, Z. Zhou, J. Niu, L. Li, Y. Wang, J. Su, J. Li, X. Wang, W. Wang, W. Wang, J. Sun, O. M. Yaghi, *Science* **2018**, *361*, 48–52; c) A. M. Evans, L. R. Parent, N. C. Flanders, R. P. Bisbey, E. Vitaku, M. S. Kirschner, R. D. Schaller, L. X. Chen, N. C. Gianneschi, W. R. Dichtel, *Science* **2018**, *361*, 52–57.

[5] a) K. Geng, T. He, R. Liu, K. T. Tan, Z. Li, S. Tao, Y. Gong, Q. Jiang, D. Jiang, *Chem. Rev.* **2020**, *120*, 8814–8933; b) N. Huang, P. Wang, D. Jiang, *Nat. Rev. Mater.* **2016,** *1*, 16068; c) D. Rodríguez-San-Miguel, C. Montoro, F. Zamora, *Chem. Soc. Rev.* **2020**, *49*, 2291−2302; d) W. K. Haug, E. M. Moscarello, E. R. Wolfson, P. L. McGrier, *Chem. Soc. Rev.* **2020**, *49*, 839–864.

[6] a) M. S. Lohse, T. Bein, *Adv. Funct. Mater.* **2018**, *28*, 1705553; b) R. Liu, K.T. Tan, Y. Gong, Y. Chen, Z. Li, S. Xie, T. He, Z. Lu, H. Yang, D. Jiang, *Chem. Soc. Rev.* **2021,** *50*, 120-242; c) S. Xu, Q. Zhang, *Mater. Today Energy* **2021,** *20*, 100635; d) H. Vardhan, A. Nafady, A.M. Al-Enizi, S. Ma, *Nanoscale* **2019,** *11*, 21679-21708; e) L. Ma, X. Feng, S. Wang, B. Wang, *Mater. Chem. Front.* **2017,** *1*, 2474-2486.

[7] a) S. Wan, J. Guo, J. Kim, H. Ihee, D. Jiang, *Angew. Chem. Int. Ed.* **2008**, *47*, 8826−8830; *Angew. Chem.* **2008**, *120*, 8958–8962; b) Z. Li, Y. Zhang, H. Xia, Y. Mu, X. Liu, Chem. *Commun.* **2016**, *52*, 6613–6616; c) A. M. Evans, I. Castano, A. Brumberg, L. R. Parent, A. R. Corcos, R. L. Li, N. C. Flanders, D. J. Gosztola, N.C. Gianneschi, R. D. Schaller, W. R. Dichtel, *J. Am. Chem. Soc.* **2019,** *141*, 19728–19735; d) F. Yu, W. Liu, S.-W. Ke, M. Kurmoo, J.-L. Zuo, Q. Zhang, *Nat. Commun.* **2020,** *11*, 1-6. e) J. W. Crowe, L. A. Baldwin, P. L. McGrier, *J. Am. Chem. Soc.* **2016**, *138*, 10120−10123; f) T. Jadhav, Y. Fang, W. Patterson, C.-H. Liu, E. Hamzehpoor, D. F. Perepichka, *Angew. Chem. Int. Ed.* **2019,** *58*, 13753–13757; *Angew. Chem.* **2019,** *131*, 13891–13895; g) S. Haldar, D. Chakraborty, B. Roy, G. Banappanavar, K. Rinku, D. Mullangi, P. Hazra, D. Kabra and R. Vaidhyanathan, *J. Am. Chem. Soc.* **2018,** *140*, 13367–13374; h) S. Ding, M. Dong, Y. Wang, Y. Chen, H. Wang, C. Su, W. Wang, J. *Am. Chem. Soc.* **2016**, *138*, 3031–3037; i) Z. Li, N. Huang, K. H. Lee, Y. Feng, S. Tao, D. Jiang, Y. Nagao, S. Irle, D. Jiang, *J. Am. Chem. Soc.* **2018**, *140*, 12374−12377.

[8] a) X. Chen, M. Addicoa, E. Jin, L. Zhai, H. Xu, N. Huang, Z. Guo, L. Liu, S. Irle, D. Jiang, *J. Am. Chem. Soc.* **2015,** *137*, 3241–3247; b) X. Li, Q. Gao, J. Wang, Y. Chen, Z. Chen, H. Xu, W. Tang, K. Leng, G. Ning, J. Wu, Q. Xu, S. Y. Quek, Y. Lu, K. P. Loh, *Nat. Commun.* **2018**, 9, 2335.

[9] a) F. J. Uribe-Romo, C. J. Doonan, H. Furukawa, K. Oisaki, O. M. Yaghi, *J. Am. Chem. Soc.* **2011**, *133*, 11478−11481; b) L. Stegbauer, K. Schwinghammer, B. V. Lotsch, *Chem. Sci.* **2014,** 5, 2789–2793.

[10] a) S. Dalapati, E. Jin, M. Addicoat, T. Heine, D. Jiang, *J. Am. Chem. Soc.* **2016**, *138*, 5797−5800; b) E. Jin, J. Li, K. Geng, Q. Jiang, H. Xu, Q. Xu, D. Jiang, *Nat. Commun.* **2018**, *9*, 4143; c) H. Ding, J. Li, G. Xie, G. Lin, R. Chen, Z. Peng, C. Yang, B. Wang, J. Sun, C. Wang, *Nat. Commun.* **2018**, *9*, 5234.

[11] A. C. Sedgwick, L. Wu, H.-H. Han, S. D. Bull, X.-P. He, T. D. James, J. L. Sessler, B. Z. Tang, H. Tian, J. Yoon, *Chem. Soc. Rev.* **2018,** 47, 8842-8880.

[12] B. P. Biswal, S. Valligatla, M. Wang, T. Banerjee, N. A. Saad, B. M. K. Mariserla, N. Chandrasekhar, D. Becker, M. Addicoat, I. Senkovska, R. Berger, D. N. Rao, S. Kaskel, X. Feng, *Angew. Chem. Int. Ed.* **2019**, *58*, 6896-6900; *Angew. Chem.* **2019**, *131*, 6970-6974.

[13] a) S. Dalapati, S. Jin, J. Gao, Y. Xu, A. Nagai, D. Jiang, *J. Am. Chem. Soc.* **2013,** *135*, 17310−17313; b) G. Lin, H. Ding, D. Yuan, B. Wang, C. Wang, *J. Am. Chem. Soc.* **2016**, *138*, 3302−3305; c) G. Das, B. P. Biswal, S. Kandambeth, V. Venkatesh, G. Kaur, M. Addicoat, T. Heine, S. Verma, R. Banerjee, *Chem. Sci.*, **2015**, *6*, 3931–3939.

Entry for the Table of Contents

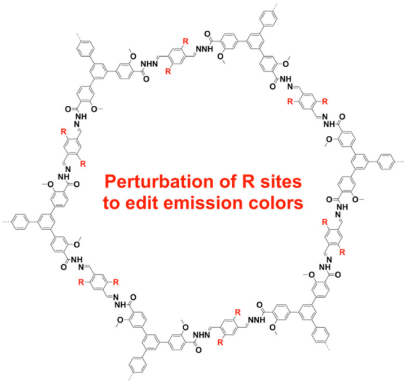

Neon lights: Topology-directed polymerization enables the construction of highly emissive stable covalent organic frameworks linked by hydrazone bond. Perturbation of pore wall surface site can tune the emission to achieve three primary colors of light, rendering the materials able to edit various emission colors by organizing different surface sites onto the pore wall.

Institute and/or researcher Twitter usernames: @jiang_donglin